https://doi.org/10.5194/hess-2022-103
Preprint. Discussion started: 17 March 2022

Hydrology and Earth System Sciences
Discussions
Open Access
EGU

Characterizing basin-scale precipitation gradients in the Third Pole region and associated determinants

Yaozhi Jiang[1], Kun Yang[1, 2, *], Hua Yang[2], Hui Lu[1], Yingying Chen[2], Xu Zhou[2], Jing Sun[1], Yuan Yang[3], Yan Wang[4]

[1] Department of Earth System Science, Ministry of Education Key Laboratory for Earth System Modeling, Institute for Global Change Studies, Tsinghua University, Beijing, China.

[2] National Tibetan Plateau Data Center, State Key Laboratory of Tibetan Plateau Earth System, Environment and Resources, Institute of Tibetan Plateau Research, Chinese Academy of Sciences, Beijing, China.

[3] Institute of Science and Technology, China Three Gorges Corporation, Beijing, China

[4]Key Laboratory of Land Surface Pattern and Simulation, Institute of Geographic Science and Natural Resources Research, Chinese Academy of Sciences, Beijing 100101, China

Corresponding author: Kun Yang (yangk@tsinghua.edu.cn)

https://doi.org/10.5194/hess-2022-103
Preprint. Discussion started: 17 March 2022

Hydrology and Earth System Sciences
Discussions
Open Access
EGU

Abstract: Altitudinal precipitation gradient plays an important role in the interpolation of precipitation in the Third Pole (TP) region, where the topography is very complex but in-situ data are very sparse. This study proves that the altitude dependence of precipitation in the TP can be reasonably reproduced by high-resolution atmospheric simulations. Results show that most of the sub-basins have positive relative precipitation gradients (RPGs, precipitation changes per 100 m elevation difference relative to basin-average precipitation) among the 388 sub-basins of the TP. The RPGs derived from annual mean precipitation range from about -5.00% in the Himalaya region to more than 20.00% in the Qaidam Basin. Generally, the RPGs are large in the center of TP, but small in the east and west, meanwhile, they are large in winter and spring but small in summer and autumn. Such a spatiotemporal pattern is related to the local weather conditions. Further analyses demonstrate that the RPGs have strong negative correlations with relative humidity but strong positive correlations with wind speed, which is because dry air tends to reach saturation at high altitudes, while stronger wind can bring more humid air to high altitudes. These findings provide useful information for the interpolation of precipitation within and beyond the TP, and are expected to provide some references to further hydrometeorological applications.

Keywords: precipitation gradient; the Third Pole; high-resolution atmospheric simulation; spatiotemporal variability

https://doi.org/10.5194/hess-2022-103
Preprint. Discussion started: 17 March 2022

1. Introduction

Gridded precipitation is a key input for many hydrological and ecological models when applied to a regional study. Typically, the spatial distribution of precipitation in a region can be obtained by interpolating the in-situ data. In regions with flat terrain and dense rain gauge networks, different interpolation methods (e.g. Thiessen polygons, inverse distance weighting, Kriging) can result in similar distributions of precipitation. In mountainous regions, precipitation has great spatial heterogeneity and rain gauges are usually sparse and located in lowland areas, where the weather conditions are much different from those in high altitudes (Chen et al., 2012; Daly et al., 2002). Sparse rain gauges with limited spatial representativeness make the interpolation of precipitation challenging in these regions. Relations between precipitation and other environmental factors (e.g. topography and vegetation) play an important role in the interpolation of precipitation, especially in mountainous regions. Among the many environmental factors, altitude is considered to have significant impacts on the distribution of precipitation. Several widely-used interpolation models have taken the altitude as a covariant, such as PRISM (Daly et al., 1997) and ANUSPLIN (Hutchinson, 1991). Moreover, some studies have reported that taking the precipitation gradient into account in hydrological modeling results in better simulations (Immerzeel et al., 2014; Li Wang et al., 2018; Zhang et al., 2015). Therefore, quantifying the precipitation gradient is greatly important in mountainous regions.

As the main source of many large rivers in Asia, the Third Pole (TP) is a typical mountainous region in the world, characterized by complex terrain and high altitude. Due to the sparse and unevenly-distributed rain gauge networks, studies on the altitude dependence of precipitation are mostly in the eastern TP (Cuo and Zhang, 2017; Guo et al., 2016) and some sub-regions, such as the Himalaya (Ouyang et al., 2020; Salerno et al., 2015; Yang et al., 2018), the Qilian Mountains (Chen et al., 2018; Lei Wang et al., 2018), the Yarlung Tsangpo River basin (Sun et al., 2021) and the Hengduan Mountains (Yu et al., 2018). Moreover, the precipitation gradients obtained in these studies are usually based on rain gauge data, which may misrepresent precipitation gradient due to the poor representativeness of rain gauges (they are usually located in valleys or lowland areas). For most parts of the TP, particularly the central and western TP, the precipitation gradients remain unknown. Besides, the precipitation gradients may vary with different seasons and years due to the changes in weather and

https://doi.org/10.5194/hess-2022-103
Preprint. Discussion started: 17 March 2022

meteorological conditions, and the temporal variability of the precipitation gradient in the TP has not been investigated yet.

In previous studies, satellite precipitation products also are used to calculate the precipitation gradients (Liu et al., 2011). However, the satellite products contain large uncertainties and are less accurate in complex-terrain regions (Derin and Yilmaz, 2014; Henn et al., 2018; Shen et al., 2014; Xu et al., 2017). In the western TP, where solid precipitation is dominated, the satellite products cannot reproduce the actual spatial variability of precipitation (Li et al., 2020). Therefore, obtaining the precipitation gradients based on satellite products seems to be undesirable in these regions.

Recently, high-resolution atmospheric simulations have made great progress in the TP and its surroundings and many atmospheric simulation-based precipitation datasets have been arising (Maussion et al., 2014; Pan et al., 2012; Wang et al., 2020; Zhou et al., 2021). The atmospheric simulations are constrained by a set of physical processes and thus can well represent the influence of topography on precipitation distribution when integrated with high resolution (Lundquist et al., 2019; Y. Wang et al., 2018). Previous studies have demonstrated the potential ability of atmospheric simulations (especially convective-permitting simulations) in capturing spatial variability of precipitation in the TP, e.g. Zhou et al. (2021) found that the downscaled precipitation of ~3 km horizontal resolution, which is generated by the WRF model (Skamarock et al., 2008), have high correlations with observations in the TP; Gao et al. (2020) found that a convective-permitting simulation could better reproduce the precipitation distribution and further resulted in better snow cover simulation than satellite-based products in the southeastern TP. Similar results were also reported in the Himalaya regions (Collier and Immerzeel, 2015; Ouyang et al., 2021) and western TP (Pritchard et al., 2019). These studies indicate that high-resolution model simulations can be alternative sources for obtaining the precipitation gradients in the TP, particularly in regions like the western TP with almost no rain gauges located.

Additionally, to depict well the spatial and temporal variabilities of precipitation gradient in a specific region, it is important to find its key factors, especially in regions where reliable high-resolution precipitation datasets are unavailable. Previous studies mainly focused on the influence of static topographic parameters (e.g. altitude, slope, aspect and exposure) on precipitation distribution (Basist et al., 1994; Diodato, 2005; Sevruk, 1997; Singh et al., 1995). Nevertheless, some studies observed remarkable seasonal variations of precipitation gradients (Li and Fu, 1984; Putkonen, 2004;

https://doi.org/10.5194/hess-2022-103
Preprint. Discussion started: 17 March 2022

Wulf et al., 2010; Zhao et al., 2011), which implies that precipitation gradients can be related to weather conditions. However, very limited works have been done to investigate the relationships between precipitation and meteorological factors.

Therefore, the objective of this study is to investigate the spatial and temporal variability of precipitation gradients in the TP based on a high-resolution atmospheric simulation-based dataset. In addition, the relations between precipitation gradients and two meteorological factors (i.e. humidity and wind speed) will also be discussed, to explore whether these factors can provide potential auxiliary information for adjusting the precipitation gradient in a region.

2. Description of datasets

2.1. Precipitation datasets

The dataset used to quantify the precipitation gradients is produced by Jiang et al. (2021). It covers the whole TP and is generated by combing the ERA5 reanalysis (Hersbach et al., 2021) with the high-resolution simulated precipitation produced by Zhou et al. (2021). Three main steps are involved to produce this dataset: first, a short-term high-resolution WRF simulation with a horizontal resolution of 1/30° is conducted; second, the precipitation from ERA5 is corrected with the high-resolution simulated precipitation, meanwhile, a convolutional neural network-based model is also trained using the high-resolution simulated precipitation; third, the corrected ERA5 precipitation is downscaled to a resolution of 1/30° using the trained model. This downscaled precipitation shows similar performance in describing the spatial variability of precipitation to the WRF simulations produced by Zhou et al. (2021), while it has a wide temporal coverage spanning 39 years from 1980 to 2018, which allows us to investigate the interannual variations of precipitation gradients in the TP. For convenience, this downscaled precipitation is called ERA5_CNN hereafter.

To validate whether the ERA5_CNN dataset can represent the altitude dependence of precipitation in the TP, observations from five rain gauge networks are used in this study. Details about the rain gauge networks are given in Table 1 and their locations are shown in Fig. 1.

https://doi.org/10.5194/hess-2022-103
Preprint. Discussion started: 17 March 2022

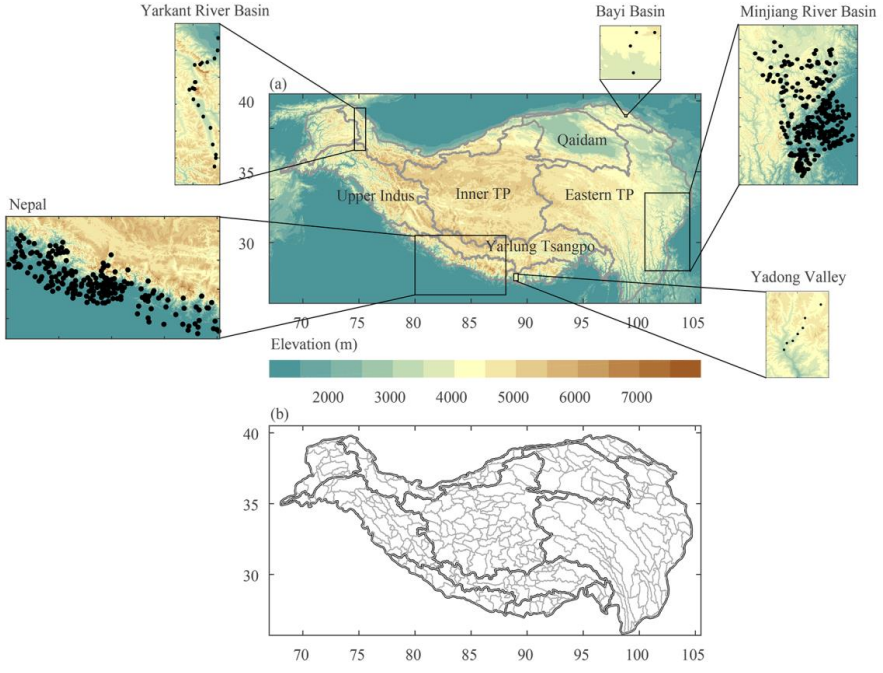

Figure 1 (a) Topography of the Third Pole (TP) region and the boundaries of five sub-regions of the TP, along with the distribution of the five rain gauge networks. (b) The boundary of the 388 sub-basins in the TP. Figure 1b shows the area above 2500 m a.s.l. The boundaries of the TP and the five sub-regions are derived from Zhang (2019).

Table 1 Basic information about the five rain gauge networks used in this study.

Rain gauge network	Temporal coverage	Number of gauges	Source
Yarkant River basin	2014.01-2015.12	28	(Kan et al., 2018)
Bayi basin	2018.07-2018.09	4	(Han et al., 2020)
Mingjiang River basin	2017.01-2017.12	375	The Hydrological Bureau of the Ministry of Water Resources (MWR) in China
Yadong valley	2018.07-2018.09	9	This study
Nepal	2014.01-2016.12	283	The Department of Hydrology and Meteorology (DHM) in Nepal

2.2. Other datasets

The elevation data used in this study is from the NASA Shuttle Radar Topographic Mission

https://doi.org/10.5194/hess-2022-103
Preprint. Discussion started: 17 March 2022


Hydrology and Earth System Sciences
Discussions
Open Access
EGU

(SRTM), which provides global digital elevation data (DEM) at a resolution of 90 m. The 90-m DEM is resampled to 1/30° to match the horizontal resolution of the precipitation data. The resample is achieved by averaging the elevation of all 90-m grids within a 1/30° grid.

In this study, the altitude dependences of precipitation from IMERG (Integrated Multi-satellite Retrievals for Global Precipitation Measurement; Huffman et al., 2019) and HAR V2 (High Asia Refined Analysis version 2; Wang et al., 2020) are also investigated. IMERG is the latest generation of global satellite-based precipitation product. The final run version of IMERG V06 with a horizontal resolution of 0.1° is used in this study, which has applied gauge observations to correct the satellite estimates. The HAR V2 is produced by dynamically downscaling the ERA5 reanalysis using the WRF model. It also covers the whole TP but has a coarser horizontal resolution (10 km) than ERA5_CNN.

The ERA5 reanalysis data of near-surface humidity and wind speed are also used to explore the relations between precipitation gradients and meteorological factors.

3. Method

The precipitation gradients are calculated based on a linear regression between precipitation and altitudes, which can be expressed as follow:

$$P = a \times H + b\,, \tag{1}$$

Where P is precipitation, H is altitude, a is the absolute precipitation gradient within a specific region, and b is the intercept of the regression equation. In this study, the regression equation is fitted in each sub-basin of the TP. The geometries of 388 sub-basins (shown in Fig. 1b) are derived from the HydroATLAS database (Linke et al., 2019), which provides twelve nested levels of sub-basins for the global. The level 6 sub-basins are applied in this study and these sub-basins have areas ranging from 2.91 km^2 to 120135.00 km^2. The relatively small size of these sub-basins can ensure that the grids used to fit the equations are dominated by similar prevailing winds. Moreover, the basin-scale precipitation gradients are easier to be applied for hydrological applications than gridded precipitation gradients. For a sub-basin, the precipitation gradient is estimated only when the following three principles are met: (1) the number of grids within the sub-basin should not be less than 10; (2) the standard deviation of altitude within the sub-basin should not be less than 50 m; (3) the p-value of the Student's t-test for the regression equation should be less than 0.05.

https://doi.org/10.5194/hess-2022-103
Preprint. Discussion started: 17 March 2022


Hydrology and Earth System Sciences
Discussions
Open Access
EGU

Although the ERA5_CNN shows good performance in representing spatial variability of precipitation, it has a systematic bias in the TP (Jiang et al., 2021). Therefore, we adopt the relative precipitation gradient (RPG) to represent the altitude dependence of precipitation in this study. The RPG is calculated as follows:

$$RPG = \frac{a}{\bar{P}} \times 100\%, \quad (2)$$

Where a is the absolute precipitation gradient from Equation (1) and $\bar{P}$ is the basin mean precipitation. For calculating the RPG, $\bar{P}$ should be greater than 0.1 mm.d^{-1}.

4. Results

4.1. Validation of the altitude dependence of precipitation

The altitude dependence of precipitation from ERA5_CNN is compared with that from rain gauge data in five networks, as shown in Fig. 2. For comparison, the altitude dependences of precipitation from IMERG and HAR V2, are also investigated. To eliminate the influence of systematic bias in precipitation products, relative precipitation amounts are adopted in Fig. 2, in which the actual precipitation amounts from either rain gauge data or products in each elevation zone are normalized by their mean precipitation amount in the region.

As shown in Fig. 2a, in the Yarkant River basin, all three datasets can generally reproduce the observed precipitation variability. ERA5_CNN is the most consistent with rain gauge data, while IMERG shows a slower change with altitude below 2800 m a.s.l. and HAR V2 presents a sharper precipitation gradient above 4000 m a.s.l. In the Bayi Basin (Fig. 2b), altitude dependence of precipitation from ERA5_CNN is almost the same to that from rain gauge data. For the other two datasets, precipitation from IMERG decreases with altitude beyond 4600 m a.s.l., while precipitation from HAR V2 has similar magnitudes at different altitudes. In the Minjiang River Basin (Fig. 2c), precipitation from rain gauge data increases with altitude below 1200 m a.s.l., then decreases with altitude between 1200-3200 m a.s.l., then increases again with altitude above 3200 m a.s.l. Among the three gridded datasets, ERA5_CNN shows the most similar altitude dependence of precipitation to rain gauge data. HAR V2 can also generally reproduce the observed pattern but change slowly with altitude above 1600 m a.s.l. However, precipitation from IMERG shows little change with respect to different altitudes in the Minjiang River Basin. In the Yadong Valley (Fig. 2d), ERA5_CNN can generally

https://doi.org/10.5194/hess-2022-103
Preprint. Discussion started: 17 March 2022

Hydrology and Earth System Sciences
Discussions
Open Access
EGU

reproduce altitude dependence of precipitation from rain gauge data, with precipitation firstly increasing slowly and then decreasing sharply with altitude, although the altitude of the precipitation maximum in ERA5_CNN is higher than that in rain gauge data. precipitation from HAR V2 shows a similar pattern to that of rain gauge data above 3600 m a.s.l, however, it decreases with altitude below 3600 m a.s.l, which is different from the rain gauge data. The altitude dependence of precipitation from IMERG is completely opposite to the observed one in the Yadong Valley. In Nepal (Fig. 2e), precipitation amounts from rain gauge data show high variability between different altitude zones. Generally, it increases with altitude below 1200 m a.s.l. and then decreases with altitude above this level. It can be seen from Fig. 2e that ERA5_CNN can better represent the altitude dependence of observed precipitation than the other two products, particularly in reproducing the large variability of precipitation.

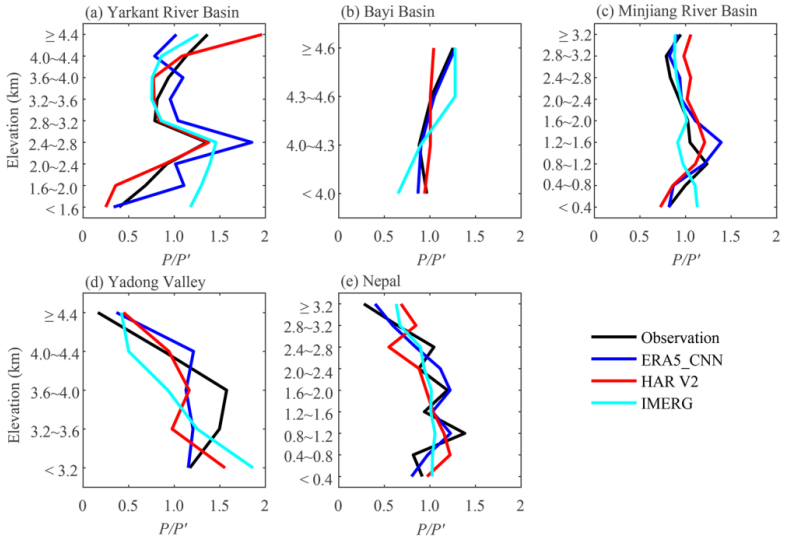

Figure 2 Comparison between the altitude dependence of relative precipitation from ERA5_CNN, IMERG and HAR V2 and that from gauge observations in five networks. *P/P´* denotes the ratio of precipitation amount (*P*) in each elevation zone to the mean precipitation amount (*P´*) at all gauge locations.

Overall, ERA5_CNN can reasonably represent the altitude dependence of precipitation in the TP and shows better performance than the widely-used IMERG and HAR V2. Therefore, it can be used to quantify the spatial and temporal variability of RPGs in the TP.

https://doi.org/10.5194/hess-2022-103
Preprint. Discussion started: 17 March 2022

Hydrology and Earth System Sciences
Discussions
Open Access
EGU

4.2. Spatial patterns of RPGs

Figure 3 shows the spatial distribution of RPGs (precipitation change per 100-m altitude difference relative to basin-average precipitation) that are calculated based on annual mean precipitation of 1980-2018 in the TP, along with the correlations between annual mean precipitation and altitudes in each sub-basin. It can be seen from Fig. 3a that there are strong correlations between precipitation and altitude in many sub-basins, of absolute correlations larger than 0.50 at about 55% of the sub-basins. Therefore, it is feasible to interpolate precipitation based on precipitation gradients in the TP.

As shown in Fig. 3b, most sub-basins (80.67% of the total) have positive RPGs. In some specific regions, such as the Qilian Mountains (Wang et al., 2009; Han et al., 2020) and some small basins in the southern TP (Li Wang et al., 2018; Zeng et al., 2021; Zhang et al., 2015) where the observed precipitation generally increases with altitude, our study reports consistent results. The sub-basins with negative RPGs are mainly distributed along the Himalayas. This is consistent with previous studies (Andermann et al., 2011; Bookhagen and Burbank, 2006; Chen et al., 2020; Salerno et al., 2015; Tang et al., 2018), which have demonstrated that precipitation decreases with altitude above 2500 m a.s.l. in this region.

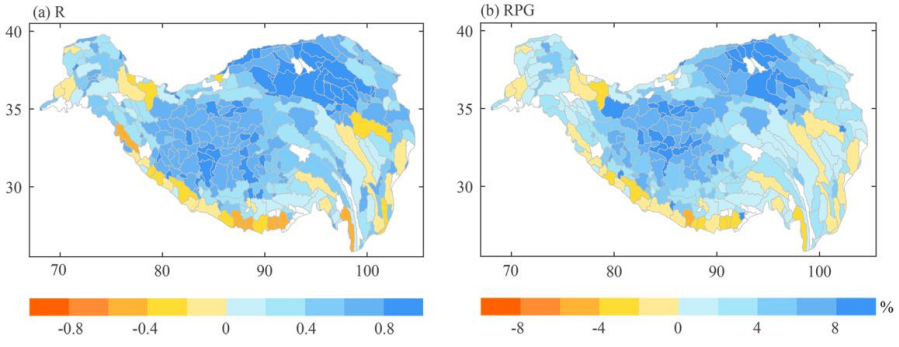

Figure 3 (a) Spatial distribution of correlations between the annual average precipitation and altitude for all grids within each basin. (b) Spatial distribution of relative precipitation gradients (RPGs, precipitation change per 100 m altitude difference relative to basin-average precipitation). The RPGs are calculated based on annual precipitation averaged from 1980 to 2018. The sub-basins with weak relationships between precipitation and altitude or no data value of RPG are filled with white

https://doi.org/10.5194/hess-2022-103
Preprint. Discussion started: 17 March 2022


Hydrology and Earth System Sciences
Discussions
Open Access
EGU

The average RPG across all the sub-basins of the TP is 4.25%. However, the RPGs show great spatial variability, ranging from -5.23% to more than 20.00%. Generally, the RPGs are small in the western and eastern but large in the central TP, which is corresponding to the spatial patterns of precipitation (i.e. wet east and west, dry center) reported in Li et al. (2020), indicating that RPGs may have negative correlations with humidity. Quantitatively, the average RPGs within five sub-regions of the TP are shown in Table 2. In terms of the RPGs derived from annual precipitation, the Qaidam Basin has the largest value of 11.26%, followed by the Inner TP with a value of 7.08%, and then the Upper Indus with a value of 3.17%. The Yarlung Tsangpo River Basin and the eastern TP (covering the Yellow, the Yangtze, the Lancang and the Nu River Basin) have RPGs of 3.00% and 2.90%, respectively. Generally, the spatial pattern of RPG shown in our study is in agreement with the result of Guo et al. (2016), which pointed out that large precipitation gradients in the Qaidam Basin but small in the Hengduan Mountains in the southeastern TP.

Table 2 The RPGs (%, relative precipitation gradients, i.e. precipitation changes per 100 m altitude difference relative to basin-average precipitation) averaged across the sub-basins within the five sub-regions and the whole TP with respect to different seasons.

	Eastern TP	Yarlung Tsangpo	Inner TP	Qaidam	Upper Indus	Whole TP
Winter	4.01	6.04	13.20	7.53	3.65	5.06
Spring	2.76	6.04	8.99	11.69	3.90	5.11
Summer	3.21	2.87	6.67	10.47	2.81	4.20
Autumn	2.42	3.51	7.39	11.37	3.02	4.33
Annual	2.90	3.00	7.08	11.26	3.17	4.25

.4.3 Temporal variation of RPGs

4.3.1 Seasonal patterns

The RPGs at each basin are also calculated based on the seasonal mean precipitation, and presented in Fig. 4, to explore the seasonality of RPGs. In winter, precipitation in some sub-basins is

https://doi.org/10.5194/hess-2022-103
Preprint. Discussion started: 17 March 2022

Hydrology and Earth System Sciences
Discussions
Open Access
EGU

very small, therefore, the RPGs are not calculated in these basins and masked with white. The general spatial patterns of RPGs in all four seasons are similar to those calculated based on annual precipitation (Fig. 3b). However, the magnitudes of RPGs vary significantly in different seasons. Generally, RPGs in spring and autumn are larger than those in summer, which is especially true in the central TP. In winter, although many sub-basins are masked as no data, most of the remaining sub-basins have the largest RPGs among the four seasons. Table 2 shows that the RPGs averaged across all the sub-basins in the TP are 5.06% in winter, 5.11% in spring, 4.20% in summer and 4.33% in autumn. Generally, the five sub-regions also have larger RPGs in cold seasons than in warm seasons.

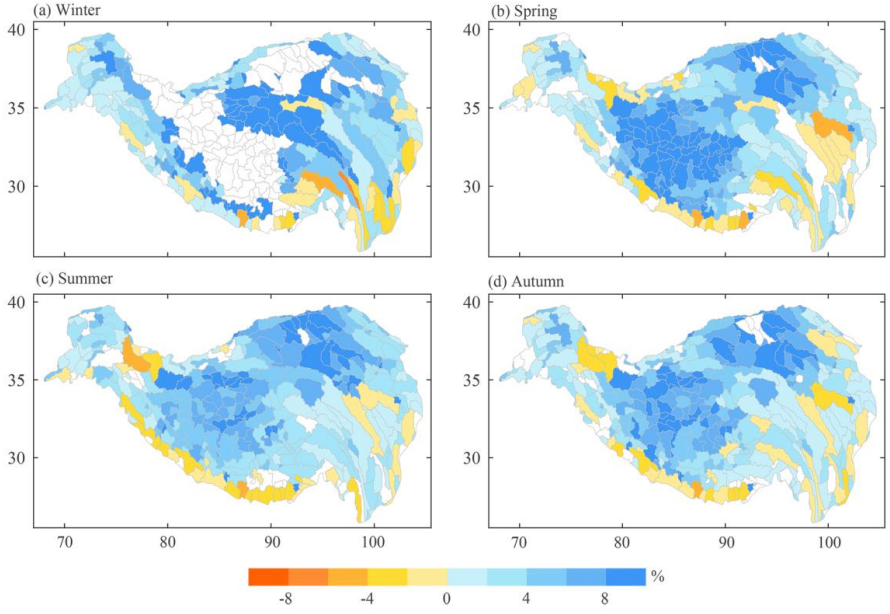

Figure 4 Spatial distribution of RPGs in (a) winter (December to February), (b) spring (March to May), (c) summer (June to August) and (d) autumn (September to November). The RPGs are calculated based on seasonal precipitation averaged from 1980 to 2018.

Particularly, remarkable seasonal variation of RPGs can be found in the Himalayas. In winter, most of the sub-basins in this region have positive RPGs, however, it can be seen from Fig. 4c that this region is dominated by negative RPGs in summer. In spring and autumn (Fig. 4b and 4d), the western Himalaya has positive RPGs and the eastern Himalaya has negative RPGs. This phenomenon was also observed by Wulf et al. (2010) who found that in the northwest Himalaya the precipitation gradients are

https://doi.org/10.5194/hess-2022-103
Preprint. Discussion started: 17 March 2022

reversed between winter and summer, as well as by Putkonen (2004) who reported that in the Nepal Himalaya monsoon precipitation maximum occurs at the altitude of about 3000 m a.s.l., while precipitation continuously increases with altitude in dry seasons.

In summary, the RPGs in the TP in winter and spring are larger than those in summer and autumn. It may be undesirable to interpolate seasonal or monthly precipitation with RPGs calculated at annual scale, especially in regions (like the Himalayas) where strong seasonal variation exists in RPGs.

4.3.2 Interannual variations

The RPGs are calculated for each year from 1980 to 2018, and then the annual RPGs are averaged across all the sub-basins in the TP or within the five sub-regions. Figure 5 displays the interannual variations of RPGs in different regions of the TP. There is no significant trend in RPGs at all the sub-regions. To quantify the interannual variations of RPGs, we calculate the coefficient of variation (CV) of annual RPGs for each sub-region. All the five sub-regions and the whole TP have CV values less than 0.12, indicating that RPGs change little between different years, which can also be found in Fig. 5. Therefore, interpolating annual precipitation with RPGs calculated based on annual average precipitation or the precipitation of a given year is credible.

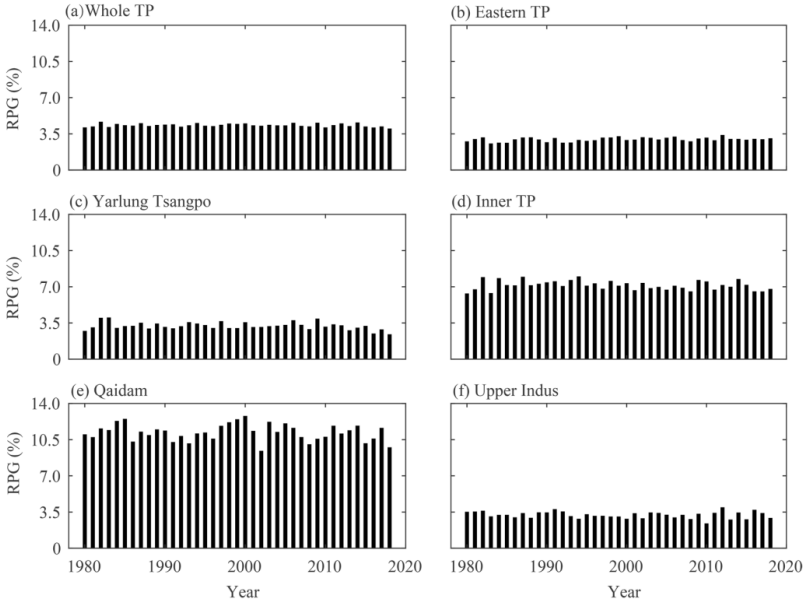

Figure 5 Interannual variations of RPGs average across the sub-basins within (a) the whole TP and (b-f)

https://doi.org/10.5194/hess-2022-103
Preprint. Discussion started: 17 March 2022

five sub-regions.

5. Discussions

As shown in Sect. 4, we can know that RPGs in the TP have great spatial and seasonal variabilities. This section discusses the potential factors that may have impacts on the spatial and temporal variabilities of RPGs. The near-surface relative humidity and wind speed are selected as the potential factors because they should be the indicators of mass and dynamic conditions for the formation of precipitation, respectively.

5.1 Relations between relative humidity and RPG

Our results show that RPGs in the TP have notable seasonal variations with large values in winter and spring but small values in summer. Similar results have been reported in the Himalayas (Putkonen, 2004), the Xinjiang region (Zhao et al., 2011) and the Qinling Mountains (Li and Fu, 1984). These studies found that the altitude with precipitation maximum in dry seasons is higher than that in wet seasons. Our results show that large RPGs mainly occur at the Qaidam basin and Inner TP that are characterized by dry air conditions. These results indicate that there may be a close relationship between RPG and humidity of air mass. Therefore, the relationships between relative humidity and RPG for annual and seasonal average precipitation are investigated. As shown in Fig. 6a-e, there are good linear relationships between relative humidity and RPGs with correlations ranging from 0.57 to 0.71. The RPGs generally decrease with increasing relative humidity for all seasons, indicating that precipitation tends to occur at lower altitudes when the relative humidity is large, which is consistent with the above results. The negative correlations between RPG and relative humidity are easy to be understood because air masses with high humidity tend to be saturated after a short uplift (see Fig. 7a).

https://doi.org/10.5194/hess-2022-103
Preprint. Discussion started: 17 March 2022

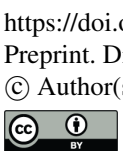

Hydrology and Earth System Sciences
Discussions
Open Access
EGU

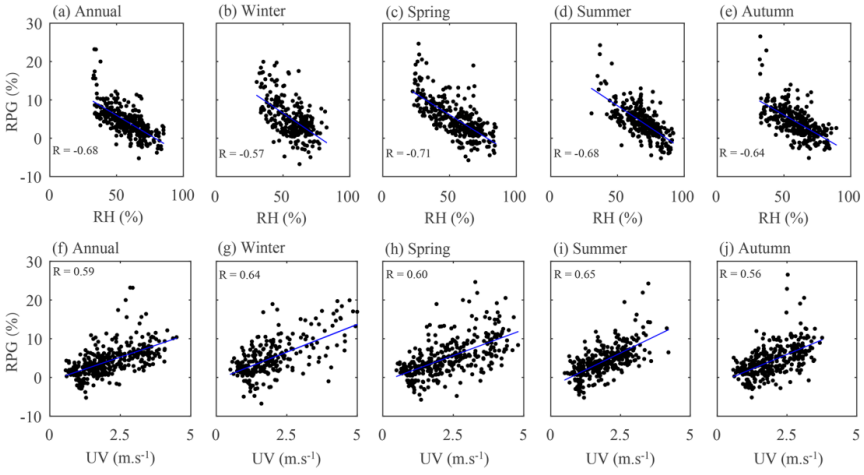

Figure 6 Relationships between RPGs and (a-e) basin-average relative humidity (RH) and (f-j) wind speed (UV).

5.2 Relations between wind speed and RPG

The relations between near-surface wind speed and RPG were also tested. RPGs linearly increase with increasing wind speed and the correlations between the two are about 0.60 for both annual and seasonal scales (Fig. 6f-j). The positive correlations between precipitation gradients and wind speed reported in this study have also been demonstrated in previous studies, e.g. Johansson and Chen (2003) found that precipitation in Sweden increases with altitude on the upwind side of mountains, based on the rain gauge observations; Hill (1983) also confirmed that wind direction and wind speed could have great impacts on the distribution of precipitation enhancement in mountainous regions. Moist air blocked by upwind barriers usually leads to enhanced precipitation in the windward slopes, which is one of the main mechanisms of orographic precipitation in mountainous regions (Houze, 2012; Roe, 2005). Thus, strong wind tends to bring more moisture to high altitudes and further results in precipitation enhancement in high altitudes, as illustrated in Fig. 7b, which is consistent with Hill (1983) and Johansson and Chen (2003).

https://doi.org/10.5194/hess-2022-103
Preprint. Discussion started: 17 March 2022

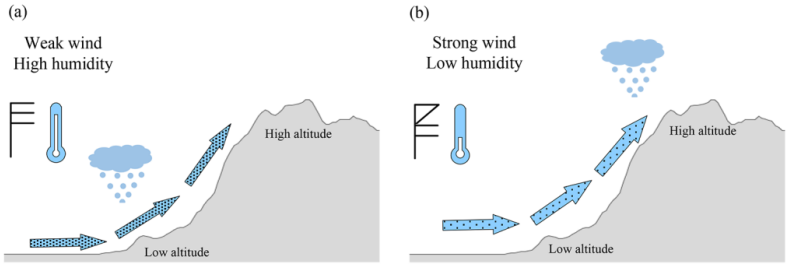

Figure 7 Schematic of the relationships between precipitation distribution along a slope and wind speed and humidity. The shadow area denotes the altitude, the size of the arrow denotes the intensity of wind, and the density of points within the arrow denote the magnitude of humidity.

6. Conclusions

The altitudinal precipitation gradient in the TP is investigated at the basin scale using a high-resolution atmospheric simulation-based precipitation dataset and its spatiotemporal variability is also analyzed.

The performance of the high-resolution atmospheric simulation-based dataset in describing the altitude dependence of precipitation is firstly validated using observations from five rain gauge networks. The results show that this dataset can reasonably reproduce the observed altitude dependence of precipitation and has higher performance than the widely-used IMERG and HAR V2 in the TP.

The relative precipitation gradients (RPGs) for annual average precipitation are calculated in 388 sub-basins of the TP. The RPG averaged across all sub-basins is 4.25%. Most sub-basins of the TP have positive RPGs and negative RPGs are mainly distributed along the Himalayas. Generally, RPGs are large in the central but small in the western and eastern TP with the largest RPGs at the Qaidam Basin. The RPGs have remarkable seasonal variations with large values in winter and spring but small ones in summer and autumn. In contrast, the RPGs have low inter-annual variability.

Further analyses show that the RPGs decrease with increasing relative humidity but increase with increasing wind speed. The linear relationships between RPGs and the two factors are strong with absolute correlations greater than 0.50 for both factors. The strong correlations suggest that relative humidity and wind speed can be potential indicators to adjust RPGs regionally.

In summary, our study quantifies the spatiotemporal variability of precipitation gradient in the TP

https://doi.org/10.5194/hess-2022-103
Preprint. Discussion started: 17 March 2022

and reveals the two meteorological factors that may affect the precipitation gradient. Nevertheless, further works need to be done to comprehensively evaluate the accuracy of the obtained precipitation gradients in the TP, which requires reliable observations, e.g. high-quality radar observation or high-density rain gauge networks.

Code and Data availability. All codes used to produce the results are available upon request to the authors. The high-resolution atmospheric simulation-based precipitation dataset that supports this study is available upon request from the authors. Relative precipitation gradients for 388 sub-basins of the TP are provided in the supplementary file.

Author contributions. Yaozhi Jiang: Conceptualization, Data curation, Investigation, Formal analysis, Methodology, Software, Visualization, Writing – original draft preparation; **Kun Yang**: Conceptualization, Funding acquisition, Project administration, Resources, Funding acquisition, Supervision, Writing – review & editing; **Hua Yang**: Conceptualization, Data curation, Writing – review & editing; **Hui Lu**: Supervision, Writing – review & editing; **Yingying Chen**: Data curation, Writing – review & editing; **Xu Zhou**: Methodology, Writing – review & editing; **Jing Sun**: Methodology, Writing – review & editing; **Yuan Yang and Yan Wang**: Writing – review & editing

Conflict of interest. The authors declare that they have no conflict of interest.

Acknowledgments. This work was supported by the Strategic Priority Research Program of Chinese Academy of Sciences (Grant No. XDA2006010201), National Science Foundation of China (Grant No. 41905087) and NSFC Basic Science Center for Tibetan Plateau Earth System (Grant No. 41988101). This is a contribution to CORDEX-FPS-CPTP. The dataset of the boundaries of the TP and its five sub-regions used in this study is provided by National Tibetan Plateau Data Center (http://data.tpdc.ac.cn)

https://doi.org/10.5194/hess-2022-103
Preprint. Discussion started: 17 March 2022

Reference

Andermann, C., Bonnet, S., and Gloaguen, R.: Evaluation of precipitation data sets along the Himalayan front, Geochemistry, Geophys. Geosystems, 12, https://doi.org/10.1029/2011GC003513, 2011.

Basist, A., Bell1, G.D., and Meentemeyer, V.: Statistical Relationships between Topography and Precipitation Patterns. J. Clim. 7, 1305–1315, 1994.

Bookhagen, B. and Burbank, D.W.: Topography, relief, and TRMM-derived rainfall variations along the Himalaya, Geophys. Res. Lett., 33, 1–5, https://doi.org/10.1029/2006GL026037, 2006

Chen, H., Yuan, W., Li, J., and Yu, R.: A possible cause for different diurnal variations of warm season rainfall as shown in station observations and TRMM 3B42 data over the southeastern Tibetan plateau, Adv. Atmos. Sci., 29, 193–200, https://doi.org/10.1007/s00376-011-0218-1, 2012.

Chen, R., Han, C., Liu, J., Yang, Y., Liu, Z., Wang, L., and Kang, E.: Maximum precipitation altitude on the northern flank of the Qilian Mountains, northwest China, Hydrol. Res., 49, 1696–1710, https://doi.org/10.2166/nh.2018.121, 2018.

Chen, Y., Sharma, S., Zhou, X., Yang, K., Li, X., Niu, X., Hu, X., and Khadka, N.: Spatial performance of multiple reanalysis precipitation datasets on the southern slope of central Himalaya, Atmos. Res., 105365, https://doi.org/10.1016/j.atmosres.2020.105365, 2020.

Collier, E. and Immerzeel, W.W.: High-resolution modeling of atmospheric dynamics in the Nepalese Himalaya, J. Geophys. Res. Atmos., 120, 9882–9896, https://doi.org/10.1038/175238c0, 2015.

Cuo, L. and Zhang, Y.: Spatial patterns of wet season precipitation vertical gradients on the Tibetan Plateau and the surroundings, Sci. Rep., 7, 1–10, https://doi.org/10.1038/s41598-017-05345-6, 2017.

Daly, C., Gibson, W.P., Taylor, G.H., Johnson, G.L., and Pasteris, P.: A knowledge-based approach to the statistical mapping of climate, Clim. Res., 22, 99–113, https://doi.org/10.3354/cr022099, 2002.

Daly, C., Taylor, G., and Gibson, W.: The Prism approach to mapping precipitation and temperature, 10th AMS Conf. Appl. Climatol., 1–4 , 1997.

Derin, Y. and Yilmaz, K.K.: Evaluation of multiple satellite-based precipitation products over complex topography, J. Hydrometeorol., 15, 1498–1516, https://doi.org/10.1175/JHM-D-13-0191.1, 2014.

https://doi.org/10.5194/hess-2022-103
Preprint. Discussion started: 17 March 2022


Hydrology and Earth System Sciences
Discussions
Open Access
EGU

Diodato, N.: The influence of topographic co-variables on the spatial variability of precipitation over small regions of complex terrain, Int. J. Climatol., 25, 351–363, https://doi.org/10.1002/joc.1131, 2005.

Gao, Y., Chen, F., and Jiang, Y.: Evaluation of a convection-permitting modeling of precipitation over the Tibetan Plateau and its influences on the simulation of snow-cover fraction, J. Hydrometeorol., 21, 1531–1548, https://doi.org/10.1175/JHM-D-19-0277.1, 2020.

Guo, X., Wang, L., and Tian, L.: Spatio-temporal variability of vertical gradients of major meteorological observations around the Tibetan Plateau, Int. J. Climatol., 36, 1901–1916, https://doi.org/10.1002/joc.4468, 2016.

Han, C., Wang, L., Chen, R., Liu, Z., Liu, J., Yang, Y., and Lv, H.: Precipitation observation network and its data application in the alpine region of Qilian Mountains (in Chinese). Resources Science. 42, 1987–1997. https://doi.org/10.18402/resci.2020.10.15, 2020.

Henn, B., Newman, A.J., Livneh, B., Daly, C., and Lundquist, J.D.: An assessment of differences in gridded precipitation datasets in complex terrain, J. Hydrol., 556, 1205–1219, https://doi.org/10.1016/j.jhydrol.2017.03.008, 2018.

Hersbach, H., Bell, B., Berrisford, P., Hirahara, S., Horányi, A., Muñoz-Sabater, J., Nicolas, J., Peubey, C., Radu, R., Schepers, D., Simmons, A., Soci, C., Abdalla, S., Abellan, X., Balsamo, G., Bechtold, P., Biavati, G., Bidlot, J., Bonavita, M., De Chiara, G., Dahlgren, P., Dee, D., Diamantakis, M., Dragani, R., Flemming, J., Forbes, R., Fuentes, M., Geer, A., Haimberger, L., Healy, S., Hogan, R.J., Hólm, E., Janisková, M., Keeley, S., Laloyaux, P., Lopez, P., Lupu, C., Radnoti, G., de Rosnay, P., Rozum, I., Vamborg, F., Villaume, S., and Thépaut, J.N.: The ERA5 global reanalysis, Q. J. R. Meteorol. Soc., 146, 1999–2049, https://doi.org/10.1002/qj.3803, 2020.

Hill, F.F.: The use of average annual rainfall to derive estimates of orographic enhancement of frontal rain over England and Wales for different wind directions, J. Climatol., 3, 113–129, https://doi.org/10.1002/joc.3370030202, 1983.

Houze, R.A.: Orographic Effects on Precipitating Clouds, Rev. Geophys., 1–47, https://doi.org/10.1029/2011RG000365.1.INTRODUCTION, 2012.

Huffman, G., Bolvin, D., Nelkin, E., and Tan, J.: Integrated Multi-satellitE Retrievals for GPM

https://doi.org/10.5194/hess-2022-103
Preprint. Discussion started: 17 March 2022

(IMERG) Technical Documentation. NASA , 2019.

Hutchinson, M.F.: The application of thin plate smoothing splines to continent-wide data assimilation, In: Jasper JD (ed.) BMRC Research Report No. 27, Data Assimilation Systems, 104–113, 1991.

Immerzeel, W.W., Petersen, L., Ragettli, S., and Pellicciotti, F.: The importance of observed gradients of air temperature and precipitation for modeling runoff from a glacierized watershed in the Nepalese Himalayas, Water Resour. Res., 5375–5377, https://doi.org/10.1002/2013WR014979.Reply, 2014.

Jiang, Y., Yang, K., Shao, C., Zhou, X., Zhao, L., and Chen, Y.: A downscaling approach for constructing high-resolution precipitation dataset over the Tibetan Plateau from ERA5 reanalysis, Atmos. Res., 256, 105574, https://doi.org/10.1016/j.atmosres.2021.105574, 2021.

Johansson, B. and Chen, D.: The influence of wind and topography on precipitation distribution in Sweden: Statistical analysis and modelling, Int. J. Climatol., 23, 1523–1535, https://doi.org/10.1002/joc.951, 2003.

Kan, B., Su, F., Xu, B., Xie, Y., Li, J., and Zhang, H.: Generation of High Mountain Precipitation and Temperature Data for a Quantitative Assessment of Flow Regime in the Upper Yarkant Basin in the Karakoram, J. Geophys. Res. Atmos., 123, 8462–8486, https://doi.org/10.1029/2017JD028055, 2018.

Li, D., Yang, K., Tang, W., Li, X., Zhou, X., and Guo, D.: Characterizing precipitation in high altitudes of the western Tibetan plateau with a focus on major glacier areas, Int. J. Climatol., 1–14, https://doi.org/10.1002/joc.6509, 2020.

Li, Z. and Fu, B.: Characteristics of climate in Qinling Mountains // Monography of Montain Climate, Meteorological Press, Beijing , 1984.

Linke, S., Lehner, B., Ouellet Dallaire, C., Ariwi, J., Grill, G., Anand, M., Beames, P., Burchard-Levine, V., Maxwell, S., Moidu, H., Tan, F., and Thieme, M.: Global hydro-environmental sub-basin and river reach characteristics at high spatial resolution, Sci. Data, 6, 1–15, https://doi.org/10.1038/s41597-019-0300-6, 2019.

Liu, J., Chen, R., Qin, W., and Yang, Y.: Study on the vertical distribution of precipitation in mountainous regions using TRMM data, Adv. water Sci., 22, 447–454, 2011.

https://doi.org/10.5194/hess-2022-103
Preprint. Discussion started: 17 March 2022

Lundquist, J., HugHes, M., Gutmann, E., and KapnicK, S.: Our skill in modeling mountain rain and snow is bypassing the skill of our observational networks, Bull. Am. Meteorol. Soc., 2473–2490, https://doi.org/10.1175/BAMS-D-19-0001.1, 2019.

Maussion, F., Scherer, D., Mölg, T., Collier, E., Curio, J., and Finkelnburg, R.: Precipitation seasonality and variability over the Tibetan Plateau as resolved by the high Asia reanalysis, J. Clim., 27, 1910–1927, https://doi.org/10.1175/JCLI-D-13-00282.1, 2014.

Ouyang, L., Lu, H., Yang, K., Leung, L.R., Wang, Y., Zhao, L., Zhou, X., LaZhu, Chen, Y., Jiang, Y., and Yao, X.: Characterizing uncertainties in ground "truth" of precipitation over complex terrain through high-resolution numerical modeling, Geophys. Res. Lett., 1–11, https://doi.org/10.1029/2020gl091950, 2021.

Ouyang, L., Yang, K., Lu, H., Chen, Y., Lazhu, Zhou, X., and Wang, Y.: Ground-Based Observations Reveal Unique Valley Precipitation Patterns in the Central Himalaya, J. Geophys. Res. Atmos., 125, 1–18, https://doi.org/10.1029/2019JD031502, 2020.

Pan, X., Li, X., Shi, X., Han, X., Luo, L., and Wang, L.: Dynamic downscaling of near-surface air temperature at the basin scale using WRF-a case study in the Heihe River Basin, China, Front. Earth Sci., 6, 314–323, https://doi.org/10.1007/s11707-012-0306-2, 2012.

Pritchard, D.M.W., Forsythe, N., Fowler, H.J., O'Donnell, G.M., and Li, X.F.: Evaluation of upper indus near-surface climate representation by WRF in the High Asia Refined Analysis, J. Hydrometeorol., 20, 467–487, https://doi.org/10.1175/JHM-D-18-0030.1, 2019.

Putkonen, J.K.: Continuous snow and rain data at 500 to 4400 m altitude near Annapurna, Nepal, 1999-2001., Arctic, Antarct. Alp. Res., 36, 244–248, https://doi.org/10.1657/1523-0430(2004)036[0244:CSARDA]2.0.CO;2, 2004.

Roe, G.H.: Orographic precipitation, Annu. Rev. Earth Planet. Sci., 33, 645–671, https://doi.org/10.1146/annurev.earth.33.092203.122541, 2005.

Salerno, F., Guyennon, N., Thakuri, S., Viviano, G., Romano, E., Vuillermoz, E., Cristofanelli, P., Stocchi, P., Agrillo, G., Ma, Y., and Tartari, G.: Weak precipitation, warm winters and springs impact glaciers of south slopes of Mt. Everest (central Himalaya) in the last 2 decades (1994-2013), Cryosphere, 9, 1229–1247, https://doi.org/10.5194/tc-9-1229-2015, 2015.

Sevruk, B.: Regional dependency of precipitation-altitude relationship in the Swiss Alps, Clim. Change,

https://doi.org/10.5194/hess-2022-103
Preprint. Discussion started: 17 March 2022

36, 355–369, https://doi.org/10.1007/978-94-015-8905-5_7, 1997.

Shen, Y., Xiong, A., Hong, Y., Yu, J., Pan, Y., Chen, Z., and Saharia, M.: Uncertainty analysis of five satellite-based precipitation products and evaluation of three optimally merged multi-algorithm products over the Tibetan Plateau, Int. J. Remote Sens., 35, 6843–6858, https://doi.org/10.1080/01431161.2014.960612, 2014.

Singh, P., Ramasastri, K.S., and Kumar, N.: Topographical influence on precipitation distribution in different ranges of western Himalayas, Hydrol. Res., 26, 259–284, https://doi.org/10.2166/nh.1995.0015, 1995.

Skamarock, W.C., Klemp, J.B., Dudhia, J., Gill, D.O., Barker, D.M., Duda, M.G., Huang, X., Wang, W., and Powers, J.G.: A Description of the Advanced Research WRF Version 3 (No. NCAR/TN–475+STR), University Corporation for Atmospheric Research, https://doi.org/10.5065/D68S4MVH, 2008.

Sun, H. and Su, F.: Precipitation correction and reconstruction for streamflow simulation based on 262 rain gauges in the upper Brahmaputra of southern Tibetan Plateau, J. Hydrol., 590, 125484, https://doi.org/10.1016/j.jhydrol.2020.125484, 2020.

Tang, G., Long, D., Hong, Y., Gao, J., and Wan, W.: Documentation of multifactorial relationships between precipitation and topography of the Tibetan Plateau using spaceborne precipitation radars, Remote Sens. Environ., 208, 82–96, https://doi.org/10.1016/j.rse.2018.02.007, 2018.

Wang, Lei, Chen, R., Song, Y., Yang, Y., Liu, J., Han, C., and Liu, Z.: Precipitation–altitude relationships on different timescales and at different precipitation magnitudes in the Qilian Mountains, Theor. Appl. Climatol., 134, 875–884, https://doi.org/10.1007/s00704-017-2316-1, 2018.

Wang, Li, Zhang, F., Zhang, H., Scott, C.A., Zeng, C., and Shi, X.: Intensive precipitation observation greatly improves hydrological modelling of the poorly gauged high mountain Mabengnong catchment in the Tibetan Plateau, J. Hydrol., 556, 500–509, https://doi.org/10.1016/j.jhydrol.2017.11.039, 2018.

Wang, N., He, J., Jiang, X., Song, G., Pu, J., Wu, X., and Chen, L.: Study on the zone of maximum precipitation in the north slopes of the central Qilian Mountains (in Chinese), Journal of Glaciology and Geocryology, 31(03), 395-403, 2009.

https://doi.org/10.5194/hess-2022-103
Preprint. Discussion started: 17 March 2022

Wang, X., Tolksdorf, V., Otto, M., and Scherer, D.: WRF-based dynamical downscaling of ERA5 reanalysis data for High Mountain Asia: Towards a new version of the High Asia Refined analysis, Int. J. Climatol., 1–20, https://doi.org/10.1002/joc.6686, 2020.

Wang, Y., Geerts, B., and Liu, C.: A 30-year convection-permitting regional climate simulation over the interior western United States. Part I: Validation, Int. J. Climatol., 38, 3684–3704, https://doi.org/10.1002/joc.5527, 2018.

Wulf, H., Bookhagen, B., and Scherler, D.: Seasonal precipitation gradients and their impact on fluvial sediment flux in the Northwest Himalaya, Geomorphology, 118, 13–21, https://doi.org/10.1016/j.geomorph.2009.12.003, 2010.

Xu, R., Tian, F., Yang, L., Hu, H., Lu, H., Hou, A.: Ground validation of GPM IMERG and trmm 3B42V7 rainfall products over Southern Tibetan plateau based on a high-density rain gauge network, J. Geophys. Res., 122, 910–924, https://doi.org/10.1002/2016JD025418, 2017.

Yang, K., Guyennon, N., Ouyang, L., Tian, L., Tartari, G., and Salerno, F.: Impact of summer monsoon on the elevation-dependence of meteorological variables in the south of central Himalaya, Int. J. Climatol., 38, 1748–1759, https://doi.org/10.1002/joc.5293, 2018.

Yu, H., Wang, L., Yang, R., Yang, M., and Gao, R.: Temporal and spatial variation of precipitation in the Hengduan Mountains region in China and its relationship with elevation and latitude, Atmos. Res., 213, 1–16, https://doi.org/10.1016/j.atmosres.2018.05.025, 2018.

Zeng, C., Zhang, F., Wang, L., and Chen, D.: Summer precipitation characteristics on the southern Tibetan plateau, Int. J. Climatol., 41, E3160–E3177, https://doi.org/10.1002/joc.6914, 2021.

Zhang, F., Zhang, H., Hagen, S.C., Ye, M., Wang, D., Gui, D., Zeng, C., Tian, L., and Liu, J.: Snow cover and runoff modelling in a high mountain catchment with scarce data: effects of temperature and precipitation parameters, Hydrol. Process., 29, 52–65, https://doi.org/10.1002/hyp.10125, 2015.

Zhang, G.: Dataset of river basins map over the TP (2016). National Tibetan Plateau Data Center, https://doi.org/10.11888/BaseGeography.tpe.249465.file.CSTR: 18406.11.BaseGeography.tpe.249465.file, 2019.

Zhao, Y., Shi, F., Sheng, Y. Li, J., Zhao, Z., Han, M., and Yilihamu, Y.: Regional differentiation characteristics of precipitation changing with altitude in Xinjiang region in recent 50 years (in

https://doi.org/10.5194/hess-2022-103
Preprint. Discussion started: 17 March 2022

Chinese), Journal of Glaciology and Geocryology (in Chinese), 33, 1203–1213., 2011.

Zhou, X., Yang, K., Ouyang, L., Wang, Y., Jiang, Y., Li, X., Chen, D., and Prein, A.: Added value of kilometer-scale modeling over the third pole region: a CORDEX-CPTP pilot study, Clim. Dyn., https://doi.org/10.1007/s00382-021-05653-8, 2021.